Conformational Properties of Dendritic Homopolymers with Interacting Branching Points

Pavlos Efthymiopoulos, Marios Kosmas,* and Costas Vlahos

Chemistry Department, University of Ioannina, 45110 Ioannina, Greece

Leonidas N. Gergidis

Department of Materials Science and Engineering, University of Ioannina, 45110 Ioannina, Greece

Received May 14, 2007; Revised Manuscript Received August 30, 2007

ABSTRACT: A microscopic model is used to determine analytically the macroscopic conformational properties of dendritic polymers with interactive branching points. We describe the dependence on the number g of generations, the molecular weight N of each branch, and the functionalities f and f_c of the branching points and the core as well as the quality of the solvent. A comparison is given between the analytical results and the results from Monte Carlo simulations up to $g = 4$ and $f_c = f = 3$. Three mean square distances are calculated which determine the extension of the k shell from the origin, the sizes of the branches in each generation, and the average distance between symmetrical points on different dendrons. On the basis of these distances, the dependence on the microscopic characteristics of the dendritic polymer of the positions of the terminal groups and the size of the branches in each generation are analyzed. Effective angles between symmetrical points on different dendrons are used for the first time to describe the degree of segregation of different dendrons the possibility of entrances into the matrix of the polymer as well as the amount of the vacancies in its interior.

1. Introduction

In recent years, the scientific and technological interest for dendritic polymers which have a treelike structure built on a core star with successive generations has been increased.[1] The hyperbranched macromolecular construction of this class of macromolecules is exhibited in Figure 1 with the two-dimensional images of specific examples. A schematic presentation of dendritic polymers with $g = 4$ (Figure 1a) and $g = 3$ (Figure 1b) generations are shown. Snapshots of dendritic polymers with branches of ten units with $f = f_c = 3$ and $g = 3$ (Figure 1c) and $g = 4$ (Figure 1d) are also shown.

The functionalities of their branching points f can be the same (Figure 1a) or different (Figure 1b) from the functionality f_c of their core with the latter determining the number of dendrons starting from the center of the macromolecule. These parameters together with the molecular weight N of each branch determine the total molecular weight of the dendritic polymer

$$M = Nf_c\sum_{i=0}^{g}(f-1)^i = Nf_c\frac{(f-1)^{g+1}-1}{f-2} \qquad (1)$$

and affect its conformational properties. Two of them, which emanate from their structure and the bursting number of their branches, are first the capability of forming entrances in their exterior and cavities in their interior and second the control of the positions and the way of action of their terminal groups. Because of their capability of accepting cargos in their cavities they can be used as host systems in the controlled drug delivery processes while the controlled positions of the terminal groups determine their activity, important in many fields like catalysis or solubility.[2] Their synthesis and study becomes more difficult though, by the bursting increase of their number of monomers with the increase of their generations and functionalities. When the spacers are small and the interactions between proximate monomers large the exponential increase of their monomers with g and f and the strong excluded volume effects between them create constraints which make their study almost forbidden. Ways of overcoming the large constraints are necessary if we want to develop dendrimers of larger numbers of generations g and larger functionalities f and f_c.

Because of the compactness of the dendritic structure the initial assumption was that terminal groups occupy the periphery of the macromolecule and that the restrictive interactions lead to a completion and saturation beyond which the generations of dendrimers cannot grow further.[3] Computational support of this density saturation has been given by means of atomistic simulations of poly(amido amine) dendrimers (PAMAM) where it was found that the growth of full generations beyond $g = 10$ was prevented.[4] The terminal groups of PAMAM of 7 generations, labeled with deuterium, was also found experimentally by means of small-angle neutron scattering to be concentrated near the periphery.[5] The general assumption though that the terminal groups belong only to the external region of macromolecule has been doubted[6] and by means of molecular dynamic simulations it was found that terminal groups may belong everywhere in the interior matrix of the dendrimer as well. It was soon realized that all microscopic parameters affect the conformational properties of dendrimers and therefore the compactness and saturation of the size of these macromolecules, a rule which is more applicable to dendritic polymers of larger flexible spacers whose units have more freedom. By means of analytical models, it was found for example that the addition of flexible spacers, spreading of the density distribution to further radial distances, and reducing the excluded volume effects allows the growth of dendritic polymers to larger generations.[7] The size of the dendrimers has been found to depend on the quality of the solvent too.[8] While it increases by increasing the repulsions between the units of the polymer, a significant collapse is detected

* Corresponding author. E-mail: mkosmas@cc.uoi.gr.

10.1021/ma071081n CCC: $37.00
Published on Web 11/08/2007

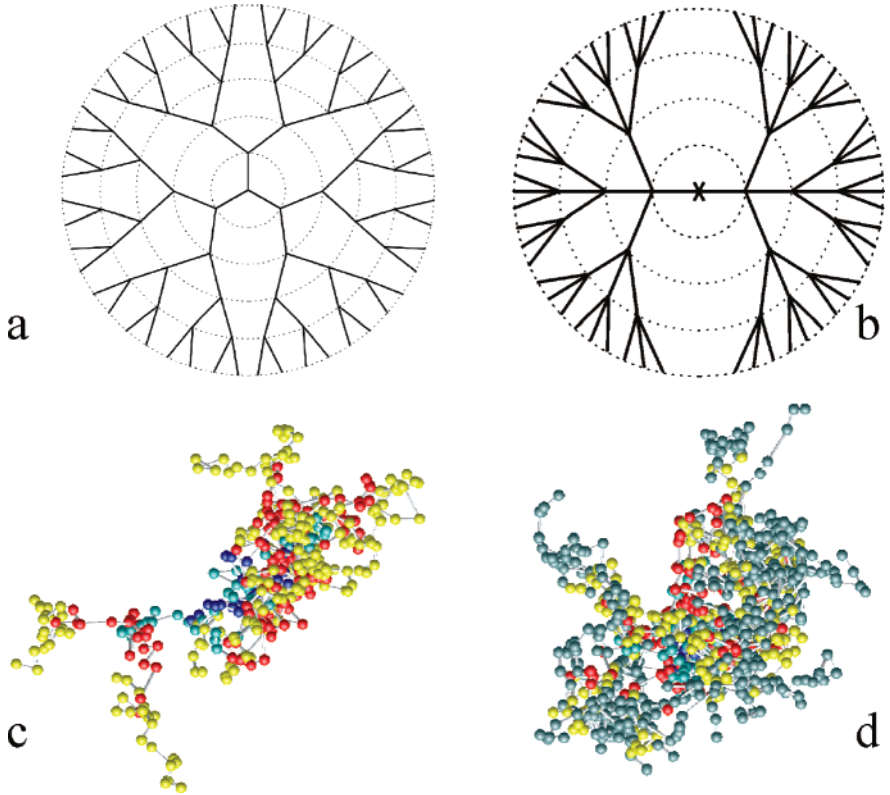

Figure 1. Dendritic polymer with (a) $g = 4$ and $f = f_c = 3$ and (b) $g = 3$, $f_c = 2$ and $f = 4$ and snapshots of dendritic polymer with branches of 10 units with $f = f_c = 3$, and $g = 3$ (c), $g = 4$ (d). Different generations are represented in color variations.

upon moving to poor solvent conditions,[9] a regularity which has also been confirmed by molecular dynamics simulations.[10] This similarity with the solution behavior of linear homopolymers is due to the homopolymer character of branches, which is expected to increase for longer spacers. Beyond the regularities, in special dendritic polymers coming from special interactions and the remaining microscopic characteristics,[11,12] the general trends in the behavior of these macromolecules are as follows: A linear chain behavior of small density for small g and compact spherelike behavior for large g has been found by means of Monte Carlo simulations.[13,14] As we go to larger dendrimers with more generations, the inner generations become progressively more extended.[15] The different primary dendrons are found to be segregated, with the amount of spatial overlap between them decreasing with increasing generation number and increasing with solvent quality.[10] By means of the diffusion coefficient measured by NMR spectroscopy and by SANS and SAXS experiments, the size of dendritic polymers has been found to depend also on the functionality of the core.[16]

The saturation and the position of the end groups are results of the effects of all microscopic characteristics of dendritic polymers and models with controlled effects of these characteristics will shed more light on the global behavior of these special class of macromolecules. Among all microscopic parameters the intensity of the interactions among the units of the dendritic polymer determine the energy of each configuration and the average conformation of the polymer. We know that intrabranch excluded volume effects determine the critical exponents and the state of the branches which can be realized to exist in expanded but also in ideal or shrinked states. The dendritic nature on the other hand is mainly affected by the rest interactions which include interbranch interactions which can also be small under Θ solvent conditions of the branches. They include the interactions of the numerous branching points too which from their nature are more voluminous and protecting even if extra bulky substituents are absent. Spacer linkers like chlorosilanes are widely used experimentally and their chemical nature is indeed different to that of spacer monomers. In the case of dendrimers with many generations the exponential increase of the number of linkers has a significant influence on their properties. The inclusion of the interactions between the branching points can furnish an estimation of the effect which the spacer linkers bring on the conformational properties of dendrimers. In an effort to study the dendritic nature in a large range of g, f, and f_c we seek a theoretical model in which by keeping the interactions between important units we reduce the excluded volume effects. The way we manage this is to keep excluded volume interactions between the members of a smaller but characteristic subset of units. We introduce thus a model of dendritic homopolymers where the dendritic nature, ensured from the connectivity term of the ideal chain, is enhanced through the inclusion only of the interactions of the branching points including the core. This choice is also justified from the fact that the functionality of the branching points, being larger or equal to 3, is certainly larger than the functionality 2 of the remaining units. This enhanced number of emerging branches makes each branching point more voluminous and interactive. The model will inspire computational as well as experimental efforts for the creation and study of dendritic polymers with controlled excluded volume effects but permitting larger functionalities and larger number of generations and branches. Synthetic efforts also, based on the creation of branches first and then connecting them into the dendritic structure, may be facilitated in more compatible states of these branches. We will describe the general regularities of the dendritic homopolymers as a function of the functionalities of the branching points and the core, the number of generations, the molecular weight of the spacers, and the quality of the solvent. We show that the

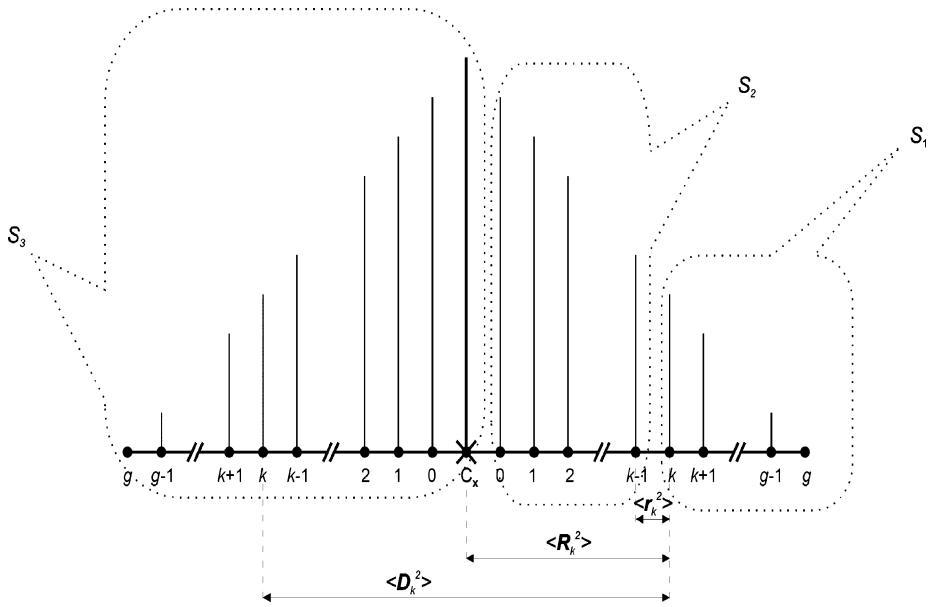

Figure 2. Two-dimensional image of a dendritic polymer of g generations. Two axis from the core point C_x to terminal points are represented with the horizontal line. The central perpendicular axis represent one of the remaining $f_c - 2$ dendrons while the remaining perpendicular lines represent subdendrons starting from the remaining $2g$ points of the two axis.

model can reproduce all known regularities but can also be extended to larger functionalities, generations, and molecular weights, which cannot be reached easily by simulation techniques. Because of the smaller number of interacting units, first-order perturbation theory in the interactions is enough to describe the macroscopic properties. Though the freedom to choose different functionalities for the various generations can easily be incorporated in our analytical treatment, we will include only the cases with two different functionalities—that of the core and that of the branching points, which we observe also in real systems and experimental studies. In section 2, we describe the microscopic model and in section 3 a comparison of the present results and those of Monte Carlo calculations up to $g = 4$ and $f = f_c = 3$ is given. In section 4, a discussion and analysis of the main tendencies of the macroscopic behavior of dendritic homopolymers is exhibited, while at the end of the paper we present a conclusion.

2.The Model

On the basis of the Gaussian model, we write the probability distribution function of the dendritic homopolymer with interacting branching points as

$$P[R(s)] = P_0[R(s)] \exp[-u\sum_i\sum_j \delta(R_i - R_j)] \qquad (2)$$

where $P_0[R(s)]$ is the ideal connectivity term of the dendritic polymer of the Gaussian type while R_i, R_j stand for the positions of all interacting branching points.[11] It is a coarse-grained model where Gaussian distribution is applied for the positions of the ends of the units. Each unit has an average length equal to the Kuhn length and contains a small number of monomeric units. The interactions between these points approaching in space are given by the 3-dimensional Dirac δ function with u being the intensity of the interactions which as in the initial Fixmann−Edwards model is proportional to the binary cluster integral.[17] It obtains positive values for repulsions between the branching points and negative values for attractions. The mean end-to-end square distances of the various parts of the dendritic polymer are obtained from expressions of the form

$$\langle R^2 \rangle = \{\int D[r(s)] R^2 P[r(s)]\} / \{\int D[r(s)] P[r(s)]\} \qquad (3)$$

where $D[r(s)]$ is the measure of the path integrals, which expresses the integrations over all points of the chain in the continuous line limit. The interacting points in the model are much fewer than the total number of the units of the chain, giving lesser effects of interactions than those of the full excluded volume problem coming from the interactions between all pairs of monomers. This can be seen from the magnitudes of the various terms in increasing powers of the u parameter. Expanding eq 2 in u and taking into account that δ functions bring into contact branching points, we obtain, by means of eq 3, the following general expression for the mean end-to-end square distances:

$$\langle R^2 \rangle = \langle R^2 \rangle_0 [1 + c_1 (uN^{-3/2}) + c_2 (uN^{-3/2})^2 + ...] \qquad (4)$$

It is easily seen from this equation that for larger molecular weight N of the branches the contribution from higher order terms becomes smaller. The combination $uN^{-3/2}$ is a small quantity for large spacer length N it decreases with N, and it is certainly much larger than the second order $(uN^{-3/2})^2$ term. We remind the reader that the corresponding parameter $uN^{1/2}$ of the full excluded volume problem applied in homopolymers or the branches of more complicated structures increases with N and explains the creation of critical exponents on N.[11] When, however, excluded volume effects are negligible like in the Θ state of branches, eq 4 offers the opportunity to describe the dendritic character of the macromolecule even from the first order u result. The constant c_1, which is expected to depend strongly on f, f_c, and g will furnish a measure of the dendritic effects. At the same time, it permits the study of dendritic polymers to higher generations and larger functionalities.

The analytical evaluation of the first order u result which includes the contribution from all loops is not trivial. We know from previous works[18] that the contribution from a loop

to the mean end-to-end square distance is not zero only when there is a common part of length C between the segment and the loop. It is equal to $(3/(2\pi l^2))^{3/2}C^2/L^{5/2}$ where L is the contour length of the loop and l the Kuhn length. Concentrating on a chain axis of the dendritic polymer which starts from the core point C_x and ends on a terminal point, we denote with $k = 0, 1, ..., g$ the end points of the $g + 1$ generations, Figure 2. In order to be able to express all nonzero interactions between pairs of branching points we sort the interacting points into three groups denoted by the symbols S_1, S_2, and S_3 shown in Figure 2, and so chosen that no interactions between the points in the same group give rise to interactive (nonzero) effects.

The first group S_1 includes the points of all external subdendrons starting from the k point including the k point. The second set S_2 includes the interior branching points of the same axis with smaller k, down to the point $k = 0$ next to the core point C_x. It includes also the branching points of all subdendrons starting from these points. The third set S_3 includes the branching points of the remaining $f_c - 1$ dendrons starting from the core including the core point C_x. For the evaluation of $\langle r_k^2\rangle$, Figure 2, the interactions between the branching points in S_1 and those of S_2 and S_3, which include the kth branch, are necessary, but no interactions between pairs in the last two sets, which do not include the segment, in either pair of points from the same set, are necessary. The various contributions can be expressed as single or multiple summations which for the case of the mean square end-to-end square distance of the kth branch lead to the form:

$$\langle r_k^2\rangle = N\left(1 + \frac{2u}{N^{3/2}}(A + B)\right)$$

where

$$A = \sum_{a=0}^{g-k}\left(\frac{(f-1)^a}{(a+k+1)^{5/2}} + (f_c - 1)\sum_{b=0}^{g}\frac{(f-1)^{a+b}}{(a+b+k+2)^{5/2}}\right)$$

$$B = \sum_{c=0}^{k-1}\sum_{a=0}^{g-k}\left(\frac{(f-1)^a}{(a+c+1)^{5/2}} + (f-2)\sum_{c'=c+1}^{g-k+2c+1}\frac{(f-1)^{a+c'-c-1}}{(a+c'+1)^{5/2}}\right) \quad (5)$$

The number of the branching points in the set S_1 in a distance $N \times \alpha$ from the k points is equal to $(f-1)^\alpha$ and this gives rise to the summation over α from zero to the remaining $g-k$ families in all four extra terms of $\langle r_k^2\rangle$. The $S_1 \times S_3$ interactions between branching points in the first and the third sets are included in the first A term, where its first part stands for the interactions of all S_1 points with the core while the second part of A counts for the interactions of S_1 with all the remaining S_3 points included in the $f_c - 1$ dendrons, except the core. The B term of $\langle r_k^2\rangle$ describes $S_1 \times S_2$ interactions. Its first part stands for the interactions of the S_1 points with the points of the k included in S_2 while its second part includes the interactions of S_1 points with the remaining S_2 points. This expression is used to find and plot the general tendencies of the size of spacers.

The second interesting property which we evaluate is the mean square distance between the core and the end of the k branch, which is given by

$$\langle R_k^2\rangle = N\left((k+1) + \frac{2u}{N^{3/2}}((k+1)^2A + C + D + E)\right)$$

where

$$C = \sum_{c=0}^{k-1}\sum_{a=0}^{g-k}\left(\frac{(c+1)^2(f-1)^a}{(a+c+1)^{5/2}} + (f-2)\sum_{c'=0}^{g-k+c}\frac{(c+1)^2(f-1)^{a+c'}}{(a+c+c'+2)^{5/2}}\right)$$

$$D = \sum_{c=0}^{k-1}\left((c+1)^{-1/2} + (f-2)\sum_{c'=0}^{g-1-c}\frac{(c+1)^2(f-1)^{c'}}{(c+c'+2)^{5/2}} + (f_c-1)\sum_{b=0}^{g}\left(\frac{(c+1)^2(f-1)^b}{(b+c+2)^{5/2}} + (f-2)\sum_{c'=0}^{g-1-c}\frac{(c+1)^2(f-1)^{b+c'}}{(b+c+c'+3)^{5/2}}\right)\right)$$

$$E = \sum_{d=0}^{k-2}\sum_{c=0}^{d}\left((c+1)^{-1/2} + (f-2)\left(\sum_{c'=0}^{g-2-d} + \sum_{c'=0}^{g-1+c-d}\right)\frac{(c+1)^2(f-1)^{c'}}{(c+c'+2)^{5/2}} + (f-2)^2\sum_{c'=0}^{g-2-d}\sum_{c''=0}^{g-1+c-d}\frac{(c+1)^2(f-1)^{c'+c''}}{(c+c'+c''+3)^{5/2}}\right) \quad (6)$$

The A term represents the effects from the $S_1 \times S_3$ interactions on $\langle R_k^2\rangle$ and its expression is given in eq 5, while the remaining C, D, and E terms describe the $S_1 \times S_2$, $S_2 \times S_3$ and $S_2 \times S_2$ interactions respectively. The two parts of the C term stand for the interactions of the S_1 points with the k points of S_2 on the same axis and the remaining points of S_2 respectively, while the D term of $S_2 \times S_3$ interactions contains four parts the two first of which describe the interactions of the two subsets of S_2 with the core while the last two those with the remaining points of the $f_c - 1$ dendrons. The four parts of the E term describe the interactions between pairs of points in the S_2 set which consists of two subsets, those of the k axis and the remaining points. Equation 6 is used for the evaluation and analysis of the positions $\langle R_g^2\rangle$ of the terminal groups ($k = g$) given in section 4.

For the mean square diameter $\langle D_k^2\rangle$, between two k points at different dendrons, Figure 2, two k axis are necessary, leaving the S_3 subset to contain the points of the remaining $f_c - 2$ dendrons starting from the core. Using primes for the second k axis and the symmetrical S_1' and S_2' subsets we take for the mean square end-to-end distances of the k diameters the following expression

$$\langle D_k^2\rangle = N\left(2(k+1) + \frac{2u}{N^{3/2}}(F + 2C + 2G + 2H + 2I + 2J + 2K + L)\right)$$

where

$$F = \sum_{a=0}^{g-k}\sum_{a'=0}^{g-k}\frac{(2(k+1))^2(f-1)^{a+a'}}{(a+a'+2(k+1))^{5/2}}$$

$$G = \sum_{a=0}^{g-k}\left(\frac{(k+1)^2(f-1)^a}{(a+k+1)^{5/2}} + (f_c-2)\sum_{c=0}^{g}\frac{(k+1)^2(f-1)^{a+c}}{(a+c+k+2)^{5/2}}\right)$$

$$H = \sum_{c=0}^{k-1}\sum_{a=0}^{g-k}\left(\frac{(c+k+2)^2(f-1)^a}{(a+c+k+2)^{5/2}} + (f-2)\sum_{c'=0}^{g-1-c}\frac{(c+k+2)^2(f-1)^{a+c'}}{(a+c+c'+k+3)^{5/2}}\right)$$

$$I = \sum_{c=0}^{k-1}\left((c+1)^{-1/2} + (f_c-2)\sum_{b=0}^{g}\frac{(c+1)^2(f-1)^b}{(b+c+2)^{5/2}} + (f-2)\sum_{c'=0}^{g-1-c}\frac{(c+1)^2(f-1)^{c'}}{(c+c'+2)^{5/2}} + (f_c-2)(f-2)\sum_{b=0}^{g}\sum_{c'=0}^{g-1-c}\frac{(c+1)^2(f-1)^{b+c'}}{(b+c+c'+3)^{5/2}}\right)$$

$$J = \sum_{d=0}^{k-2}\sum_{c=0}^{d}\left((c+1)^{-1/2} + (f-2)\left(\sum_{c'=0}^{g-k+1+d} + \sum_{c'=0}^{g-k-c+d}\right)\frac{(c+1)^2(f-1)^{c'}}{(c+c'+2)^{5/2}} + (f-2)^2\sum_{c'=0}^{g-k+1+d}\sum_{c''=0}^{g-k-c+d}\frac{(c+1)^2(f-1)^{c'+c''}}{(c+c'+c''+3)^{5/2}}\right)$$

$$K = \sum_{d=0}^{k-2}\sum_{c=0}^{k-2-d}\left((c+2\mathrm{d}+3)^{-1/2} + (f-2)\left(\sum_{c'=0}^{g-1-d} + \sum_{c'=0}^{g-c-d-2}\right)\frac{(c+2\mathrm{d}+3)^2(f-1)^{c'}}{(c+c'+2\mathrm{d}+4)^{5/2}} + (f-2)^2\sum_{c'=0}^{g-1-d}\sum_{c''=0}^{g-c-d-2}\frac{(c+2\mathrm{d}+3)^2(f-1)^{c'+c''}}{(c+c'+c''+2\mathrm{d}+5)^{5/2}}\right)$$

$$L = \sum_{c=0}^{k-1}\left((2c+2)^{-1/2} + 2(f-2)\sum_{c'=0}^{g-1-c}\frac{(2c+2)^2(f-1)^{c'}}{(2c+c'+3)^{5/2}} + (f-2)^2\sum_{c'=0}^{g-1-c}\sum_{c''=0}^{g-1-c}\frac{(2c+2)^2(f-1)^{c'+c''}}{(2c+c'+c''+4)^{5/2}}\right) \quad (7)$$

The F term describes the interactions between the S_1 and S_1' sets while the G term those between the S_3 set which includes the core and the remaining $f_c - 2$ dendrons not shown in Figure 2 and the sets S_1 and S_1' respectively. The H term stands for the interactions between the S_1 and S_2' as well as the S_1' and S_2 sets while the I term includes the pairs from the S_3 and S_2 and S_3 and S_2' sets. The C term (eq 6) describes the interactions $S_1 \times S_2$ and $S_1' \times S_2'$ while the J term the $S_2 \times S_2$ and $S_2' \times S_2'$ interactions. The remaining L and K terms describe the interactions $S_2 \times S_2'$ of the subdendrons starting from symmetrical and nonsymmetrical points of these two sets, including the corresponding axis points, respectively. Proper checks for the correctness of $\langle R_k^2\rangle$, $\langle r_k^2\rangle$, and $\langle D_k^2\rangle$ are successful. For example for $f_c = f = 2$ and $g = 0$, eqs 6, 5, and 7 reproduce the linear and star polymer cases respectively. The expression, eq 7 of $\langle D_k^2\rangle$ together with those of $\langle R_k^2\rangle$ are used to describe in section 4 the angles θ_k between the two equal sides $\langle R_k^2\rangle^{1/2}$ of a triangle whose third side is equal to $\langle D_k^2\rangle^{1/2}$. Plots of interesting cases are also given and analyzed in section 4.

3. Comparison with Monte Carlo Simulations

Our analytical results are compared with off-lattice Monte Carlo simulations for the first members of trifunctional dendritic polymers. We consider trifunctional dendritic homopolymers of different generations g equal to 1, 2, 3, and 4. Each of the $3[2^{g+1}\text{-}1]$ branches of the macromolecule contains N beads where the distance between neighboring beads is not constant but follows a Gaussian distribution with mean-root-square value l equal to the Kuhn length. For simplicity l is taken equal to one as in the analytical model which brings the analytical and the Monte Carlo methods very close. The central unit of the zeroth generation is the common origin of coordinates and is assigned as the unit $3[2^{g+1} - 1] + 1$. The end units of the macromolecule, the respective of each internal generation and the central unit interact through the Lennard-Jones potentials

$$U(R_{ij})/k_BT = 4(\epsilon/k_BT)[(\sigma/R_{ij})^{12} - (\sigma/R_{ij})^6] \quad (8)$$

where R_{ij} is the separation distance between units i and j. To reproduce the excluded volume interactions we adopt for the interaction energy ϵ between units and the steric parameter σ considered the same for all units the previously reported set of Lennard-Jones parameters ($\epsilon/k_BT = 0.1$, $\sigma = 0.8$).[12,19] Interactions are considered only between the branching points and the core as in the analytical model while all the rest units do not feel the extra Lennard-Jones interaction. Snapshots are given for the cases with $f = f_c = 3$, $N = 10$, and $g = 3$ and $g = 4$ in Figure 1, parts c and d. Dendritic homopolymers with branch length N=5, 10, 15, and 20 units are simulated. The properties of interest are the mean end-to-end square distances of the branches, of the extensions of the branching points and the diameters of symmetric points shown in Table1. The high efficient Pivot algorithm is used for the Monte Carlo sampling. Other conformations are generated by selecting a bond vector in the previous conformation and resampling its components from an appropriate Gaussian distribution. The rest of the beads on the selected branch and the units on the following arms are rotated according to three randomly chosen Euler angles. The metropolis energy criterion is used to test the acceptance or rejection of the new trial configuration. Forty independent runs are performed. Each run attempts from 40×10^6 to 10^8 Monte Carlo steps after appropriate thermalization. The properties are first averaged over all conformations in each run, and then the mean values and the standard deviations are determined from the 40 independent runs. Our simulation results for the specific choice of the potential parameters are presented in Table 1, in addition to the analytical results found for the value of $u = 0.4$. The specific choice of u in the repulsive region is done for the largest possible approach of the results of the two methods. This is permissible since small variations of u do not alter the tendencies in the properties as it is shown in the u dependence of properties in Figure 4b. The relative error of the calculated conformational properties in Table 1 varies between 0.8 and 6.8%, decreasing generally for higher values of N. It exceeds the value 6.8% only for the diameters $\langle D_i^2\rangle^{1/2}$ obtaining the largest value 11.5% only for the first diameter $\langle D_o^2\rangle^{1/2}$ due probably to the constraints of the interior region of the macromolecule. An estimation though of the correctness of both

Table 1. Analytical Results (Top Row) for $u = 0.4$ and Off-Lattice MC (Bottom Row) up to Generation $g = 4$ and $f_c = f = 3$

g		$N = 5$	$N = 10$	$N = 15$	$N = 20$
1	$\langle r_0^2\rangle^{1/2}$	2.426	3.260	3.938	4.521
		2.464 ± 0.133	3.556 ± 0.214	4.234 ± 0.154	4.871 ± 0.220
	$\langle r_1^2\rangle^{1/2}$	2.361	3.226	3.916	4.504
		2.462 ± 0.085	3.528 ± 0.180	4.203 ± 0.142	4.832 ± 0.165
	$\langle R_1^2\rangle^{1/2}$	3.430	4.610	5.570	6.394
		3.489 ± 0.116	5.009 ± 0.173	5.955 ± 0.178	6.870 ± 0.250
	$\langle D_0^2\rangle^{1/2}$	3.488	4.640	5.590	6.410
		3.490 ± 0.383	4.973 ± 0.524	6.030 ± 0.456	6.945 ± 0.510
	$\langle D_1^2\rangle^{1/2}$	4.913	6.552	7.899	9.059
		4.683 ± 0.293	6.641 ± 0.419	7.996 ± 0.487	9.325 ± 0.402
2	$\langle r_0^2\rangle^{1/2}$	2.547	3.325	3.982	4.555
		2.558 ± 0.140	3.554 ± 0.243	4.272 ± 0.110	4.854 ± 0.128
	$\langle r_1^2\rangle^{1/2}$	2.469	3.283	3.954	4.533
		2.496 ± 0.082	3.473 ± 0.181	4.185 ± 0.098	4.858 ± 0.114
	$\langle r_2^2\rangle^{1/2}$	2.373	3.232	3.920	4.507
		2.465 ± 0.078	3.462 ± 0.132	4.214 ± 0.063	4.852 ± 0.070
	$\langle R_1^2\rangle^{1/2}$	3.662	4.734	5.654	6.458
		3.620 ± 0.125	4.991 ± 0.214	6.064 ± 0.113	6.897 ± 0.140
	$\langle R_2^2\rangle^{1/2}$	4.436	5.771	6.906	7.895
		4.388 ± 0.119	6.099 ± 0.210	7.360 ± 0.106	8.403 ± 0.116
	$\langle D_0^2\rangle^{1/2}$	3.727	4.770	5.679	6.477
		3.651 ± 0.406	4.943 ± 0.376	6.087 ± 0.359	6.821 ± 0.362
	$\langle D_1^2\rangle^{1/2}$	5.333	6.780	8.054	9.177
		4.907 ± 0.326	6.646 ± 0.345	8.155 ± 0.342	9.209 ± 0.350
	$\langle D_2^2\rangle^{1/2}$	6.418	8.241	9.822	11.207
		5.857 ± 0.309	8.009 ± 0.273	9.763 ± 0.298	11.106 ± 0.290
	$g = 3$	$N = 5$	$N = 10$	$N = 15$	$N = 20$
	$\langle r_0^2\rangle^{1/2}$	2.766	3.446	4.066	4.618
		2.555 ± 0.135	3.542 ± 0.158	4.244 ± 0.131	4.901 ± 0.280
	$\langle r_1^2\rangle^{1/2}$	2.641	3.376	4.017	4.581
		2.551 ± 0.087	3.494 ± 0.102	4.278 ± 0.118	4.897 ± 0.201
	$\langle r_2^2\rangle^{1/2}$	2.506	3.302	3.967	4.543
		2.499 ± 0.073	3.488 ± 0.059	4.228 ± 0.075	4.883 ± 0.133
	$\langle r_3^2\rangle^{1/2}$	2.385	3.238	3.924	4.510
		2.487 ± 0.055	3.474 ± 0.048	4.223 ± 0.056	4.848 ± 0.083
	$\langle R_1^2\rangle^{1/2}$	4.062	4.960	5.810	6.577
		3.705 ± 0.108	5.032 ± 0.134	6.029 ± 0.139	6.949 ± 0.261
	$\langle R_2^2\rangle^{1/2}$	4.964	6.068	7.111	8.051
		4.522 ± 0.097	6.156 ± 0.116	7.438 ± 0.152	8.518 ± 0.249
	$\langle R_3^2\rangle^{1/2}$	5.601	6.931	8.159	9.257
		5.229 ± 0.092	7.088 ± 0.116	8.580 ± 0.139	9.790 ± 0.249
	$\langle D_0^2\rangle^{1/2}$	4.157	5.015	5.848	6.606
		3.658 ± 0.375	5.043 ± 0.491	6.002 ± 0.451	6.943 ± 0.072
	$\langle D_1^2\rangle^{1/2}$	6.074	7.207	8.352	9.404
		5.027 ± 0.283	6.775 ± 0.368	8.095 ± 0.420	9.337 ± 0.422
	$\langle D_2^2\rangle^{1/2}$	7.351	8.775	10.192	11.490
		6.054 ± 0.255	8.175 ± 0.307	9.858 ± 0.415	11.311 ± 0.377
	$\langle D_3^2\rangle^{1/2}$	8.231	9.981	11.663	13.186
		6.985 ± 0.251	9.412 ± 0.305	11.385 ± 0.377	13.026 ± 0.336
	$g = 4$	$N = 5$	$N = 10$	$N = 15$	$N = 20$
	$\langle r_0^2\rangle^{1/2}$	3.194	3.699	4.243	4.754
		2.660 ± 0.145	3.622 ± 0.132	4.363 ± 0.159	4.931 ± 0.160
	$\langle r_1^2\rangle^{1/2}$	2.968	3.563	4.147	4.680
		2.579 ± 0.095	3.550 ± 0.096	4.338 ± 0.111	4.895 ± 0.082
	$\langle r_2^2\rangle^{1/2}$	2.734	3.428	4.053	4.601
		2.525 ± 0.063	3.495 ± 0.055	4.255 ± 0.065	4.918 ± 0.076
	$\langle r_3^2\rangle^{1/2}$	2.545	3.323	3.982	4.554
		2.490 ± 0.048	3.478 ± 0.058	4.253 ± 0.057	4.876 ± 0.057
	$\langle r_4^2\rangle^{1/2}$	2.397	3.245	3.928	4.514
		2.466 ± 0.034	3.454 ± 0.038	4.222 ± 0.037	4.871 ± 0.040
	$\langle R_1^2\rangle^{1/2}$	4.829	5.424	6.139	6.831
		3.886 ± 0.111	5.175 ± 0.124	6.227 ± 0.135	6.954 ± 0.131
	$\langle R_2^2\rangle^{1/2}$	5.957	6.669	7.538	8.381
		4.795 ± 0.107	6.309 ± 0.108	7.629 ± 0.126	8.605 ± 0.115
	$\langle R_3^2\rangle^{1/2}$	6.731	7.609	8.638	9.626
		5.482 ± 0.089	7.261 ± 0.095	8.726 ± 0.113	9.925 ± 0.101
	$\langle R_4^2\rangle^{1/2}$	7.255	8.339	9.537	10.669
		6.051 ± 0.089	8.053 ± 0.083	9.752 ± 0.105	11.048 ± 0.097
	$\langle D_0^2\rangle^{1/2}$	4.984	5.522	6.210	6.886
		3.939 ± 0.454	5.245 ± 0.389	6.211 ± 0.484	7.075 ± 0.474
	$\langle D_1^2\rangle^{1/2}$	7.473	8.084	8.983	9.895
		5.398 ± 0.307	7.076 ± 0.322	8.421 ± 0.381	9.428 ± 0.368
	$\langle D_2^2\rangle^{1/2}$	9.095	9.863	10.975	12.098
		6.515 ± 0.273	8.485 ± 0.284	10.168 ± 0.339	11.485 ± 0.308
	$\langle D_3^2\rangle^{1/2}$	10.171	11.174	12.515	13.846
		7.408 ± 0.221	9.737 ± 0.243	11.619 ± 0.286	13.235 ± 0.276
	$\langle D_4^2\rangle^{1/2}$	10.884	12.182	13.767	15.305
		8.173 ± 0.210	10.819 ± 0.211	13.028 ± 0.261	14.781 ± 0.259

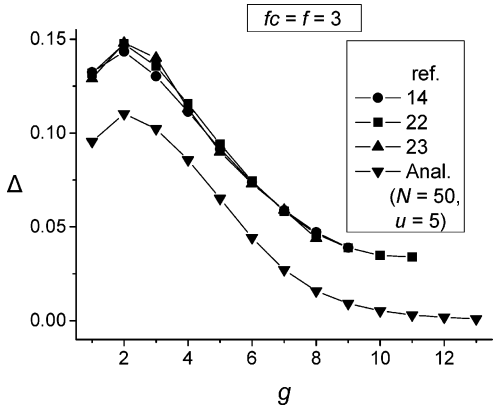

Figure 3. Comparison of the present analytical result for Δ, eq 10, with the computational results of refs 14, 22, and 23.

the analytical and the computational methods can be done by the evaluation of the expansion factors of the properties defined equal to the ratio of the property to their ideal chain values. In both methods the limit for large N tend to unity indicating the vanishing of the perturbation in the limit of very large spacers. Examples are given for the expansion factors $\{\langle R_g^2\rangle/[(g+1)N]\}^{1/2}$ of the positions of the external units expressing also the size of the macromolecule. For $g = 2$ and $g = 4$ they go as [1.15 (1.13), 1.05 (1.11), 1.03 (1.10), 1.02 (1.08)] and [1.45 (1.21), 1.18 (1.14), 1.10 (1.13), 1.07 (1.10)] for $N = 5$, 10, 15, and 20, respectively, where inside the parentheses we write the results of the computational method. The results from both methods tend to unity proving that the model applies better for higher values of N where the perturbation $uN^{-3/2}$ is smaller. The agreement of the tendencies of the results of the two techniques gives us a confidence for applying the general expressions for other functionalities f and f_c and g, N and u too, shown in Figures 4−6.

For a further comparison with existing results we employ the square root of the mean-square end-to-center distance $R = \langle R_g^2\rangle^{1/2}$ and the mean-square monomer-to-center distance $S = \langle S^2\rangle^{1/2}$ defined as[20]

$$S^2 = \frac{f_c\sum_{k=0}^{g}(f-1)^k\langle R_k^2\rangle}{f_c\sum_{k=0}^{g}(f-1)^k} = \frac{\sum_{k=0}^{g}(f-1)^k\langle R_k^2\rangle}{\frac{(f-1)^{g+1}-1}{f-2}} \qquad (9)$$

While R describes the positions of the end groups and can be determined experimentally by scattering contrast matching[5] or using SANS with deuterium labeling of the end groups, S is correlated with the distributions of all branching points, it goes as the radius of gyration of the dendritic polymer and it can be determined by using SAXS.[13,21] From S^2 obtained by means of eq 9 we calculate the quantity Δ defined as

$$\Delta = \frac{R-S}{S} \qquad (10)$$

which being rather insensitive to other microscopic details depends mainly on g[23]. Moreover our previous Monte Carlo simulations of star polymers[19] have shown that the differences in dimensionless ratios calculated at the ideal theta state and under real conditions respectively where the overlap between units is forbidden while a weak Lennard-Jones potential with $\epsilon/K_BT = 0.3$ is considered, are very small. Our predictions are depicted in Figure 3 and compared with recent simulation results existing in the literature.[14,22,23]

The similarity on the behavior of the results from the analytical work, eq 10 related to the present model with interacting branching points and the results from previous simulations on dendritic polymers with interactions from all units is satisfactory. Despite the quantitative differences between the analytical and computational results, probably caused by the different sets of interacting units adopted in the two methods the qualitative tendencies are identical. The same tendencies of the results with and without the inclusion of excluded volume effects between all units, show the importance of the interactions of the branching points. Furthermore, from our analytical result we can calculate Δ or other characteristic ratios and find their dependence on all parameters g, N, u, f_c, and f. Instead of this we explore the properties of dendritic polymers analyzing the behavior of the positions of the terminal groups, the extension from the center of the generations of dendritic homopolymers as well as the average angles between the symmetric positions of branching points on different dendrons.

4. Discussion

In this section, we use the three average distances $\langle R_k^2\rangle$, $\langle r_k^2\rangle$, and $\langle D_k^2\rangle$ in eqs 6, 5, and 7 in order to analyze the behavior of the positions of the terminal groups with $k = g$, given from their extension $\langle R_g^2\rangle^{1/2}$, and the sizes of the branches in all generations given by $\langle r_k^2\rangle^{1/2}$ ($k = 0, 1, ..., g$), as well as the angles θ_k between the two equal sides $\langle R_k^2\rangle^{1/2}$ of a triangle whose third side is equal to $\langle D_k^2\rangle^{1/2}$

$$\theta_k = \cos^{-1}\frac{2\langle R_k^2\rangle - \langle D_k^2\rangle}{2\langle R_k^2\rangle} \qquad (11)$$

Our study is based on the analysis of selected graphs chosen among many others in order to exhibit and clarify the behavior of special important properties. The behavior of the positions $\langle R_g^2\rangle$ of the terminal groups is presented in Figure 4 where characteristic families of graphs which reveal the general trends are depicted. The positions $\langle R_g^2\rangle^{1/2}$ of the terminal groups shown in Figure 4 give us also a first insight into the size of the macromolecule.

In all four families of Figure 4, we see that while for small number of generations g, $\langle R_g^2\rangle^{1/2}$ has a small increase with g indicating the linear chain behavior, a sudden increase takes place on further increase of g which marks the onset of more compact structures characterizing the dendritic nature. The present model can thus reproduce the known behaviors given previously both computationally[13−15,23] but also experimentally.[13,21] It is also in general agreement with scaling expressions giving also an increase of the size on increasing g and N.[6,10] The analytical relations given in the paper provide the possibility to describe quantitatively the dependence on all microscopic parameters. The onset of the dendritic character depends on all the remaining microscopic parameters examples of which are given in Figure 4. When the molecular weight N of each branch is smaller this expansion takes place earlier, Figure 4a, leaving the linear chain behavior only to the first members of dendrimers. The onset of dendritic character depends also on the quality of the solvent expressed with the parameter u, Figure 4b. In the good solvent region of u positive, larger u which means larger expansion of the branches and the whole molecule marks also earlier the onset of dendritic character. In the poor solvent region of u negative the initial increase with g is due to the extension of

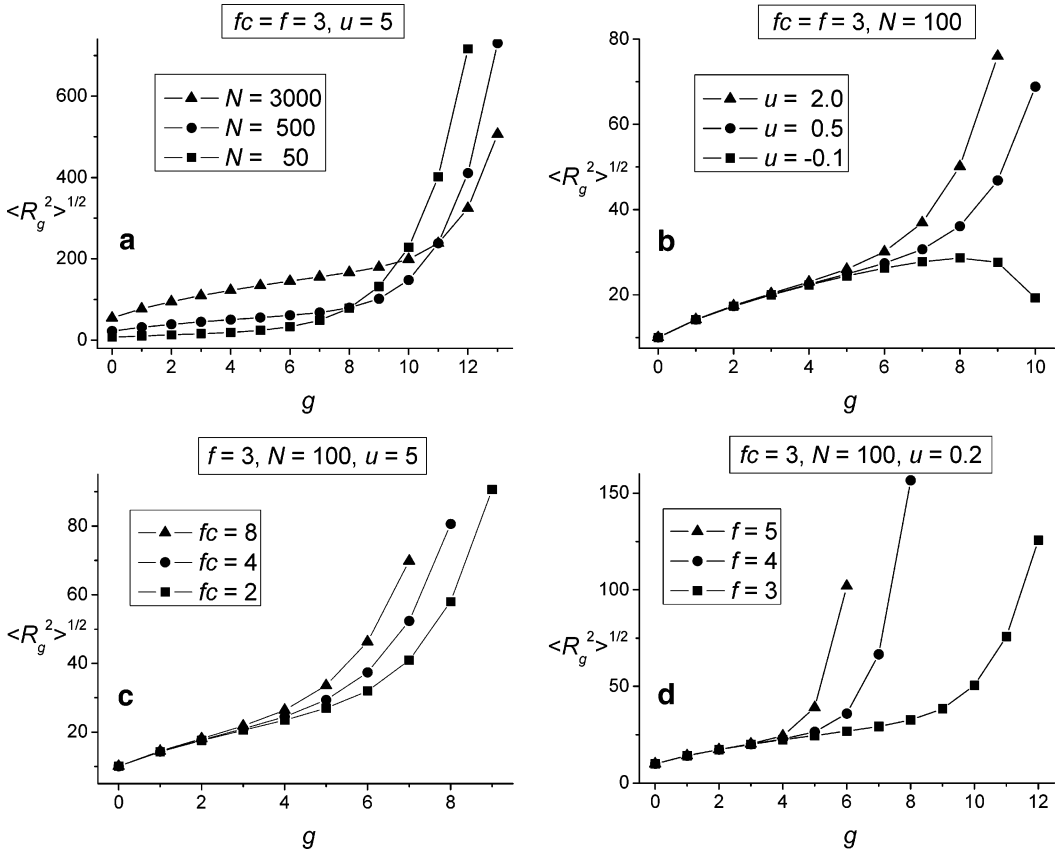

Figure 4. Positions of the terminal groups expressed by $\langle R_g^2\rangle^{1/2}$, as a function of the total number of generations g.

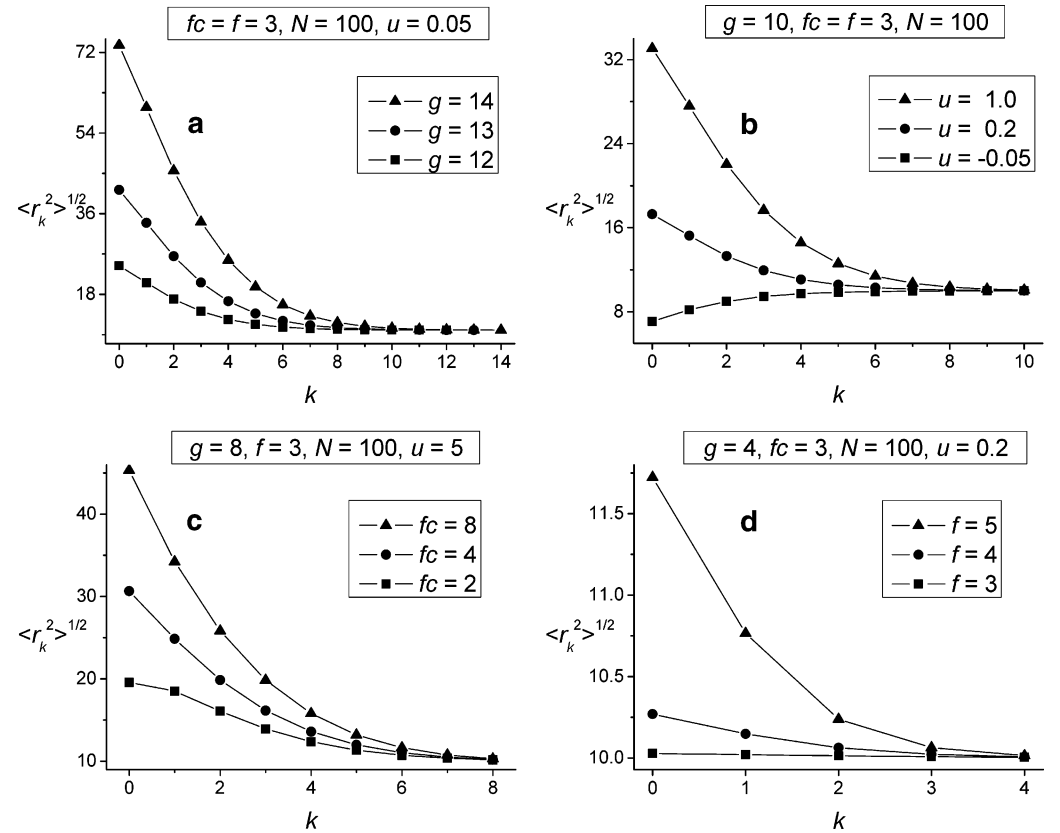

Figure 5. Dependence of the linear size $\langle r_k^2\rangle^{1/2}$ on the generation number k.

the branches which soon is neutralize by the many attractions which become effective and bring monomers closer. The number of dendrons f_c enhances also the size of the dendrimer and the onset of dendritic character, Figure 4c, its effects taking place at large numbers of generations. More obvious are the effects of the functionality f of the branching points, Figure 4d,

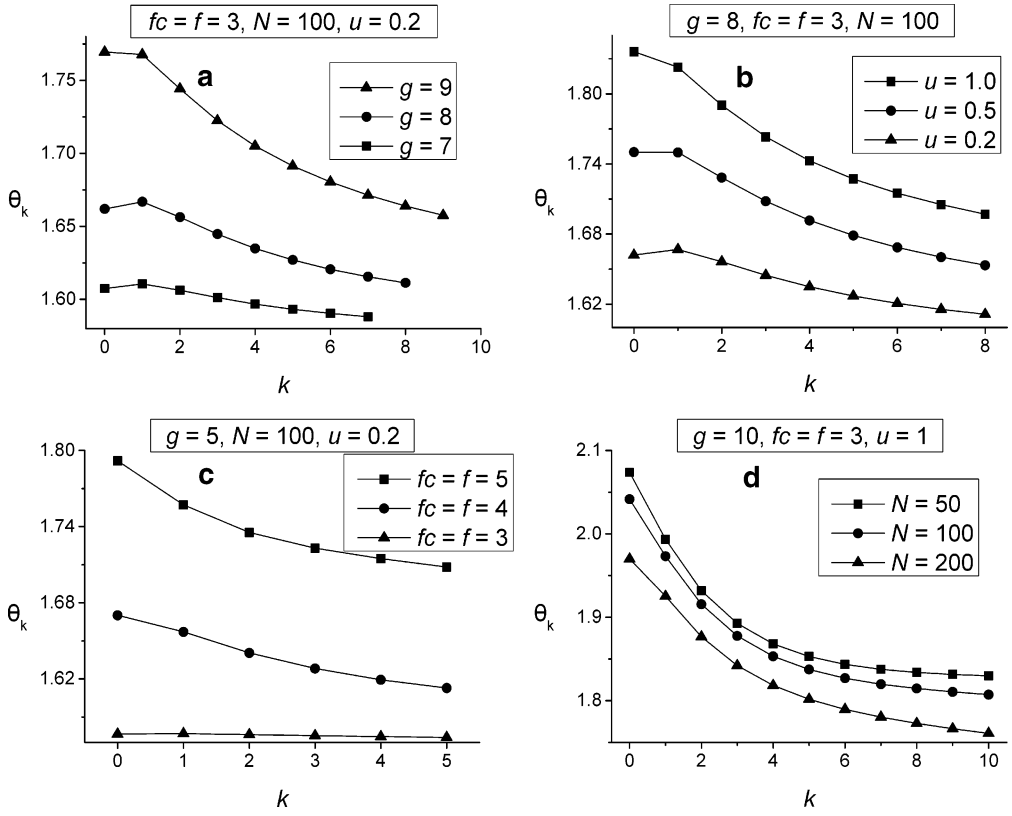

Figure 6. Dependences of the angles θ_k on the generation number k. From the four families the quantitative dependence on the parameters g, u, $f_c = f$, and N is seen.

because of the larger number of branches and monomers for larger f.

In Figure 5 a penetration to the interior of the dendritic polymer is done, where a dependence of the size $\langle r_k^2 \rangle$ on the number k of generation is given describing so both interior and exterior generations. The first thing to notice is the strong dependence on k showing the larger extension of the interior branches in agreement with the results of previous findings.[10,15] Again an analysis on the dependence on the remaining microscopic parameters can be done by means of the analytical relations given in the paper. As the total number of generations g increase, the expanding effects of the branches become stronger, enlarging even more the extension of interior branches, Figure 5a. The same trends are observed by increasing the quality of the solvent while a small inverse behavior is observed in the poor solvent region of negative u where the larger number of contacts bring opposite results, Figure 5b. Similar effects are observed by increasing the number of dendrons f_c, Figure 5c, and the functionality f of the branching points, Figure 5d.

From the diameters $\langle D_k^2 \rangle$ and the distances $\langle R_k^2 \rangle$, effective angles θ_k between symmetrical branching points on different dendrons at equal chain distances from the core are defined from their trigonometrical connection, eq 11, and also analyzed (Figure 6). The interest is that these angles characterize the openings in all generations from the first initial star to those between terminal points. We employ eq 11 and the expressions of $\langle R_k^2 \rangle$ and $\langle D_k^2 \rangle$, eqs 6 and 7, to determine the angles θ_k which we plot in Figure 6 for all $k = 0,1,2, ..., g$.

First regularity to notice from the plots of the families of Figure 6 is that the openings corresponding to larger angles θ_k are larger in the interior of the dendritic polymer at smaller k. Quantitative dependences of these openings on the microscopic parameters of the dendritic polymer are seen in this figure. We see from Figure 6a that larger g means larger angles and vacancies in agreement with previous findings.[24] The segregation of the main dendrons starting from the core, expressed also by means of the values of the θ_k angles, seen also before,[10] is increasing with g. The dependence of the angles on the quality of the solvent is exhibited in Figure 6b, where it is seen that larger u which means better solvent quality leads to larger angles and the segregation of dendrons. Larger functionalities f_c and f give also larger angles. This enlargement of angles for larger functionalities, though appearing as a paradox, is not a paradox. It can be explained by means of the constraints created because of the central structure of dendritic polymers. Larger numbers of emerging branches means more repulsions between the units of the branches which make them more extended, since they can only be expanded in the outer space. Larger extensions of the branches especially the interior ones enhance the angles between them and this is what we are seeing in Figure 6c. Finally in Figure 6d the dependence of the variation of the angles on the molecular weight N of a branch in good solvent conditions is drawn. Larger molecular weight N has as a result larger distances between the interacting branching points which leads to weaker excluded volume effects and thus to smaller θ_k angles. In the limit of infinite molecular weight N, the ideal values of the Gaussian chains $\pi/2$ (≈ 1.57 rad) for all angles is obtained. The reduction of the angles θ_k on increasing N is in agreement with previous findings on dendritic homopolymers of first generation.[12] Many other dependences can also be found and analyzed by means of the relations given in the paper which we believe will be useful to the many specific interests about these complex but interesting class of macromolecules. Keeping long flexile branches in the ideal state leaves branching points to determine the dendritic nature. This reduces the constraints among the units of the chain and therefore it will be useful both to the synthesis but also to the study of dendritic polymers of larger generations and functionalities.

5. Conclusion

Employing excluded volume interactions between the branching points we describe the conformational properties of dendritic homopolymers of g generations in terms of g, the molecular weight N of each branch, the quality of the solvent and the functionalities f_c and f of the core and the branching points. In the limit of large N first-order perturbation theory in the interaction parameter u is enough to describe properly the dendritic nature even for large number of generations and functionalities. The dependence on the microscopic parameters of the onset of dendritic behavior has been analyzed. The dendritic character starts earlier at smaller number of generations when the branch molecular weight N is smaller, when the solvent is of better quality with larger u or when the functionalities f_c and f are larger. The interior branches are more extended and this extension is bigger for larger numbers of generations, better quality of the solvent, and larger functionalities. Effective angles between symmetrical points on different dendrons are employed for the first time to the study of dendritic homopolymers and reveal that the vacancies in the interior are larger than those in the exterior, both of them increasing on increasing g or u. Increasing the functionalities of the dendritic polymer the extension of the branches becomes larger, leading also to larger segregation of dendrons and vacancies. Increasing the molecular weight of each branch the total excluded volume effects become weaker and the segregation of the dendrons decreases.

Acknowledgment. This research project is co-financed by the E.U.-European Social Fund (75%) and the Greek Ministry of Development-GSRT (25%) in the framework of the program PENED 2003 (No. 856). We thank Prof. G. Floudas and Prof. A. Charalambopoulos for useful discussions and for the computer resources used in this work.

References and Notes

(1) Fréchet, J. M. J.; Tomalia, D. A. *Dendrimers and Other Dendritic Polymers*; Wiley: Chichester, U.K., 2001. Ballauff, M.; Likos, C. N. *Angew. Chem., Int. Ed.* **2004**, *43*, 2998−3020. Boas, U.; Heegaard, P. M. H. *Chem. Soc. Rev.* **2004**, *33*, 43−63. Shi, X.; Majoros, I. J.; Baker, J. R., Jr. *Mol. Pharm.* **2005**, *2*, 278−294. Venditto, V. J.; Regino, C. A. S.; Brechbiel, M. W. *Mol. Pharm.* **2005**, *2*, 302−311.

(2) Tsiourvas, D.; Felekis, T.; Sideratou, Z.; Paleos, C. M. *Macromolecules* **2002**, *35*, 6466−6469. Lee, J. H.; Lim, Y.; Choi, J. S.; Lee, Y.; Kim, T.; Kim, H. J.; Yoon, J. K.; Kim, K; Park, J. *Bioconjugate Chem.* **2003**, *14*, 1214−1221. Chen, G.; Guan, Z. *J. Am. Chem. Soc.* **2004**, *126*, 2662−2663. Ambade, A. V.; Savariar, E. N.; Thayumanavan, S. *Mol. Pharm.* **2005**, *2*, 264−272. Gupta, U.; Agashe, H. B.; Asthana, A.; Jain, N. K. *Biomacromolecules* **2006**, *7*, 649−658. Helms, B.; Fréchet, J. M. J. *Adv. Synth. Catal.* **2006**, *348*, 1125−1148.

(3) de Gennes, P. G.; Hervet, H. *J. Phys., Lett.* **1983**, *44*, L351 − L360. Zook, T. C.; Pickett, G. T. *Phys. Rev. Lett.* **2003**, *90*, 015502.

(4) Maiti, P. K.; Cagin, T.; Wang, G.; Goddard, W. A., III. *Macromolecules* **2004**, *37*, 6236−6254.

(5) Topp, A.; Bauer, B. J; Klimash, J. W.; Spindler, R; Tomalia, D. A.; Amis, E. J. *Macromolecules* **1999**, *32*, 7226−7231.

(6) Lescanec, R. L.; Muthukumar, M. *Macromolecules* **1990**, *23*, 2280−2288.

(7) Boris, D.; Rubinstein, M. *Macromolecules* **1996**, *29*, 7251−7260.

(8) Jeong, M.; Mackay, M. E.; Vestberg, R.; Hawker, C. J. *Macromolecules* **2001**, *34*, 4927−4936.

(9) Giupponi, G.; Buzza, D. M. A. *J. Chem. Phys.* **2006**, *120*, 10290−10298.

(10) Murat, M.; Grest, G. S. *Macromolecules* **1996**, *29*, 1278−1285.

(11) Kosmas, M.; Vlahos, C.; Avgeropoulos, A. *J. Chem. Phys.* **2006**, *125*, 094908.

(12) Rangou, S.; Theodorakis, P. E.; Gergidis, L. N.; Avgeropoulos, A.; Efthymiopoulos, P.; Smyrnaios, D.; Kosmas, M.; Vlahos, C.; Giannopoulos, Th. *Polymer* **2007**, *48*, 652−663.

(13) Rathgeber, S.; Pakula, T.; Urban, V. *J. Chem. Phys.* **2004**, *121*, 3840−3853.

(14) Mansfield, M. L. *Macromolecules* **2000**, *33*, 8043−8049.

(15) Mansfield, M. L.; Klushin, L. I. *Macromolecules* **1993**, *26*, 4262−4268.

(16) Fritzinger, B.; Appelhans, D.; Voit, B.; Scheler, U. *Macromol. Rapid Commun.* **2005**, *26*, 1647−1650. Ozerin, A. N.; Svergun, D. I.; Volkov, V. V.; Kuklin, A. I.; Gordelyi, V. I.; Islamov, A. Kh.; Ozerina, L. A.; Zavorotnyuk, D. S. *J. Appl. Crystallogr.* **2005**, *38*, 996−1003.

(17) Fixman, M. *J. Chem. Phys.* **1955**, *23*, 1656−1659. Edwards, S. F. *Proc. Phys Soc.* **1965**, *85*, 613−624. Edwards, S. F. *J. Phys. A: Math. Gen.* **1975**, *8*, 1171−1177. Yamakawa, H. *Modern Theory of Polymer Solutions*; Harper and Row: New York, 1971.

(18) Vlahos, C.; Kosmas, M. *Polymer* **2003**, *44*, 503−507. Vlahos, C. H.; Kosmas, M. K. *J. Phys. A: Math. Gen.* **1987**, *20*, 1471−1483. Whittington, S. G.; Kosmas, M. K.; Gaunt, D. S. *J. Phys. A: Math. Gen.* **1988**, *21*, 4211−4216. Kosmas, M. K.; Gaunt, D. S.; Whittington, S. G. *J. Phys. A: Math. Gen.* **1989**, *22*, 5109−5116.

(19) Vlahos, C. H.; Horta, A.; Hadjichristidis, N.; Freire, J. J. *Macromolecules* **1995**, *28*, 1500−1505.

(20) Chen, Z. Y.; Cui, S.-M. *Macromolecules* **1996**, *29*, 7943−7952.

(21) Rathgeber, S.; Monkenbusch, M.; Kreitschmann, M.; Urban, V.; Brulet, A. *J. Chem. Phys.* **2002**, *117*, 4047−4062. Jana, C.; Jayamurugan, G.; Ganapathy, R.; Maiti, P. K.; Jayaraman, N.; Sood, A. K. *J. Chem. Phys.* **2006**, *124*, 204719.

(22) Mansfield, M. L.; Jeong, M. *Macromolecules* **2002**, *35*, 9794−9798.

(23) Giupponi, G.; Buzza, D. M. A. *Macromolecules* **2002**, *35*, 9799−9812.

(24) Timoshenko, E. G.; Kuznetsov, Y. A.; Connolly, R. *J. Chem. Phys.* **2002**, *117*, 9050−9062.

MA071081N